Identifies Oncogene PDRG1 as a Potential Prognostic Biomarker in Hepatocellular Carcinoma: A Study Based on Bioinformatics Analysis

Jianyang Lin (ljyang2007@126.com)
Zhenjiang First People's Hospital https://orcid.org/0000-0002-3163-8643

Xin Ding
Zhenjiang First People's Hospital

Zhihong Chen
Zhenjiang First People's Hospital

Huiwen Pan
Zhenjiang First People's Hospital

Yinyan Wu
Zhenjiang First People's Hospital

Kun Zhao
Zhenjiang First People's Hospital

Research

Keywords: PDRG1, Hepatocellular Carcinoma, Bioinformatics Analysis, Prognostic Biomarker

Posted Date: June 14th, 2021

DOI: https://doi.org/10.21203/rs.3.rs-606283/v1

Abstract

Background: Hepatocellular carcinoma (HCC) is globally recognized as one of the most frequently occurring primary malignant liver tumor, making the identification of HCC biomarkers critically important.

Methods: The gene expression and clinicopathology analysis, GO enrichment analysis (GSEA) and immune infiltration analysis are based on data obtained from The Cancer Genome Atlas (TCGA), with additional bioinformatics analyses performed. The statistical analysis was conducted in R. The protein-protein interaction (PPI) networks was constructed and the module analysis was performed using STRING and Cytoscape. Construction and evaluation of prognostic model based on PDRG1 and tumor status used nomogram and calibration.

Results: The expression of PDRG1 was significantly higher in HCC tumor tissues. High expression of PDRG1 in HCC patients was significantly correlated with poor Overall Survival and adverse clinicopathological features including advanced T stage, residual tumor, histologic grade, vascular invasion, TP53 status and AFP level. GO, GSEA revealed that PDRG1 was closely correlated with DNA repair, DNA replication and cell cycle. Spearman correlation showed high expression of PDRG1 was significantly correlated with Th2 cells level in HCC patients. Nomograms based on PDRG1 and tumor stage had good predictive performance on overall survival rates of HCC patients.

Conclusions: Our study demonstrated the potential significance of PDRG1 expression in the diagnosis and prognosis of HCC and further explored the function in HCC. Further study is still needed to confirm these results. The underlying mechanism revealed by these results provides a basis for PDRG1 as a new molecular target for the prevention and treatment of HCC.

Introduction

Hepatocellular carcinoma (HCC) is the most common primary liver cancer, representing the fifth most common cancer and the second leading cause of cancer-related mortality[1]. The mean survival time of HCC patients without intervention is estimated between 6 and 20 months. The main treatments for HCC are tumor resection, liver transplantation, microwave, radiofrequency, ablation, transcatheter arterial chemoembolization, targeted drug sorafenib and so on, but the overall survival rate of patients with HCC is still not optimistic. Thus, there is an urgent need to find effective prognostic biomarkers for HCC patients who can really benefit from curative treatment. In this study, we aim to establish a genetic marker and prognostic model that can predict the Overall Survival (OS) of HCC patients by bioinformatics methods. And this model could assist doctors to develop more individualized treatment plans.

p53 and DNA damage-regulated gene 1 (PDRG1) is a small oncogenic protein of 133 residues, locating in Exon 5 of 20q11.21[2]. In normal human tissues, PDRG1 exhibits maximal expression in the testis and minimal levels in the liver. Increased expression of PDRG1 has been detected in several tumor including lung, breast, stomach, colon, rectum and ovary cancers[3–7]. PDRG1 expression was found to be correlated with higher or more advanced tumor stages, suggesting it could play an important role in cancer progression[8]. PDRG1 expression protein has been found as an interaction target for methionine adenosyltransferase catalytic subunits MATα1 and MATα2. through this interaction, PDRG1 downregulates nuclear S-adenosylmethionine

synthesis, hence impacting epigenetic methylations. Silencing of PDRG1 expression in hepatoma cells alters their steady-state expression profile on microarrays, downregulating genes associated with tumor progression[9]. The Cancer Genome Atlas (TCGA) and Gene Expression Omnibus (GEO) database recently shared good platforms and data for genomic analysis or biological molecular markers with scientific research personnel[10]. In this research, we studied the expression level of PDRG1 in HCC patients, and then evaluated its relationship with the occurrence and development of HCC so as to see whether PDRG1 is a suitable diagnostic and prognostic biomarker for HCC.

Materials And Methods

Data Source

Gene expression data with clinical information from LIHC project (371cases, Workflow Type: HTSeq-FPKM) were collected from the Cancer Genome Atlas (TCGA). Then, level 3 HTSeq-FPKM (Fragments Per Kilobase per Million) data were transformed into TPM (transcript per million reads) for the further analyses. Unavailable or unknown clinical features were regarded as missing values. This study meets publication guidelines.

Clinical And Prognostic Statistical Analysis

The RNAseq data from TCGA and GTEx in TPM format was downloaded from UCSC XENA, which has been uniformly processed by the Toil process [11]. We compared the expression of PDRG1 in normal samples from GTEx combined with TCGA and HCC samples from TCGA by Wilcoxon rank sum test. Moreover, we also compared the expression of PDRG1 in HCC tumor issues compared with 50 pairs non-cancerous adjacent tissues using Wilcoxon signed rank test. Then, we analyzed the the relations between clinical pathologic characteristics and the expression level of PDRG1 using Wilcoxon rank sum test, Kruskal-Wallis rank sum test and logistic regression. Clinicopathological characteristics associated with Overall Survival from TCGA HCC patients using Cox regression and Kaplan-Meier method. The variables with $p < 0.1$ in Cox regression will be included in multivariate Cox regression to compare the influence of PDRG1 expression on Overall Survival of HCC patients. The cut-off value of PDRG1 expression was determined by its median value. P-values less than 0.05 were considered significant in all tests. All statistical analyses were conducted using R (version 4.0.2).

Identification Of Degs

The differentially expressed genes were analyzed by HTSeq-Counts data with DESeq2 package, considering $|logFC| \geq 2$ and p. adj < 0.05 as the threshold of differential genes (DEGs). The results of difference expression analysis are shown by volcano plot (Fig. 3A) and heatmap (Fig. 3B). A total of 436 differentially expressed genes were identified, of which 321 were up-regulated and 115 were down regulated. The top20 of DEGs including PCSK1, SPHK1, WNT7B, RP11-863K10.7, TMEM132A, ITIH5, PEBP4, PLEKHB1, TTYH1, UCHL1, SPIB, COL9A2, ZG16B, CTH, C19orf33, LAMP5, KIAA1549L, CXCL5, SIX2, PROM1.

Functional Enrichment Analysis (Go)

To predict the function of enrichment information of interactive genes of PDRG1, GO enrichment analyses were performed within Metascape. PDRG1 associated genes engaged in several BP, CCs, and MFs. We found that pattern specification process, skeletal system development, multicellular organismal homeostasis, reproductive structure development, epithelial cell differentiation, sensory organ development, metanephros development, gonadal mesoderm development, mesenchyme development, and negative regulation of cell differentiation had significant regulation by these genes. Moreover, digestive tract development, digestion, ossification, neuron fate specification, sphingolipid biosynthetic process, activation of adenylate cyclase activity, memory, stem cell proliferation, antimicrobial humoral response, regulation of blood pressure also involved in the regulation of PDRG1 interactive genes (Fig. 4A).

To further capture the relationships between the terms, a subset of enriched terms had been selected and rendered as a network plot, where terms with a similarity > 0.3 were connected by edges. We selected the terms with the best p-values from each of the 20 clusters, with the constraint that there are no more than 15 terms per cluster and no more than 250 terms in total. The network is visualized using Cytoscape, where each node represents an enriched term and is colored by its p-value (Fig. 4B).

Gene Set Enrichment Analysis (Gsea)

As many pathways contribute to tumor formation, the poor survival associated with high PDRG1 expression may be related to a number of signaling pathways activated in HCC. GSEA of differences between low and high PDRG1 expression data sets was performed to identify the key signaling pathways associated with PDRG1. We selected C2.cp.v7.0.symbols.gmt [Curated] in MSigDB Collections as the reference gene set, each gene set contains at least 10 genes and no more than 500 genes, calculation times was set as 10000. P Value less than 0.05 and False discovery rate(FDR)less than 0.25 were identified as significant differences. Statistical analysis and graphical plotting were conducted using R package ClusterProfiler (3.8.0). Among them, there are 342 datasets satisfying. We selected visual datasets were KEGG_CELL_CYCLE (NES = 2.034, p. adj = 0.004, FDR = 0.003), KEGG_DNA_REPLICATION (NES = 1.914, p. adj = 0.005, FDR = 0.004), REACTOME_DNA_REPAIR(NES = 1.655, p. adj = 0.004, FDR = 0.003) (shown in Fig. 5). The results suggest that the dataset is significantly enriched in the left red (high PDRG1 expression group).

Ppi Network Analysis

Following elimination of the DEGs with different expression tendency and isolated nodes in the network, a total of 177 nodes and 367 edges were included in the PPI network (Fig. 6). The CytoNCA plugin was used to analyze the centrality of nodes. The top 10 proteins, which were also defined as crucial proteins based on four different centrality parameters, were presented in Table 3, and they included SST, CALCA, GLP1R, AFP, FOXG1, GAGE2A, DLX2, CDX2, SIX3, FOXG1, NTS.

Table 3
The top 10 proteins ranked based on the node centrality of the PPI network

rank	Degree centrality		Betweenness centrality		Closeness centrality		Eigenvector centrality	
	Gene symbol	Expression in HCC	Gene symbol	Expression in HCC	Gene symbol	Expression in HCC	Gene symbol	Expression in HCC
1	SST	up-regulated	FOXG1	up-regulated	SST	up-regulated	SST	up-regulated
2	CHGA	up-regulated	UNC5D	down-regulated	ASCL1	down-regulated	CALCA	down-regulated
3	CALCA	down-regulated	EPHA6	up-regulated	LHX8	up-regulated	CHGA	up-regulated
4	GAD2	up-regulated	EFNA5	up-regulated	DLX2	up-regulated	TAC1	up-regulated
5	CT45A1	up-regulated	ASCL1	down-regulated	CHGA	up-regulated	DRD1	down-regulated
6	TAC1	up-regulated	PAGE1	up-regulated	GAD2	up-regulated	NTS	up-regulated
7	DRD1	down-regulated	GAGE2A	up-regulated	CDX2	up-regulated	GAST	up-regulated
8	GAST	up-regulated	GAD2	up-regulated	SIX3	up-regulated	CRHR1	up-regulated
9	GLP1R	up-regulated	SST	up-regulated	FOXG1	up-regulated	ADCY8	down-regulated
10	AFP	up-regulated	DLX2	up-regulated	DRD1	down-regulated	GLP1R	up-regulated

Analysis of immune infiltration and its correlation with PDRG1 expression

Spearman correlation was employed to show the association between the expression level (TPM) of PDRG1 and immune cell infiltration level quantified by ssGSEA in the HCC tumor microenvironment. As shown in Fig. 7A, we found that PDRG1 expression was positively correlated with NK, CD56 bright cells, Tfh, Th2 cells, and negatively correlated with neutrophils, Th17 cells, Tgd, DCs, Tcm, eosinophils, cytotoxic cells. Then we studied the relation between the expression level of PDRG1 and the infiltration levels of Th2 cells by Spearman correlation analysis (Fig. 7B). The results suggested that the expression level of PDRG1 was significantly correlated with the infiltration levels of Th2 cells. The correlation coefficient R was 0.349 ($P < 0.001$). Moreover, we analyzed the difference of Th2 cells infiltration level between PDRG1 high and low expression groups by Wilcoxon rank sum test statistical method. The results were shown in Fig. 7C. The Th2 cells infiltration level in high expression group of PDRG1 were much more than the ones in low expression group, the result was statistically significant ($p <0.001$).

Development of prognostic model based on PDRG1 and clinicopathological factors

We analyzed the diagnostic efficacy of PDRG1 in HCC patients by ROC analysis. The area under the curve (AUC) of PDRG1 (Fig. 8) was 0.962 (CI: 0.943–0.982), representing a very efficient ability to identified HCC patients from healthy people. Then, we used Kaplan-Meier Plotter to evaluate the prognostic value of PDRG1 in HCC with OS by Survminer package. High expression of PDRG1 was associated with worse OS (HR = 1.98 (1.39–2.83), p < 0.001) (Fig. 9). Moreover, we used univariate Cox regression analysis on OS in HCC patients with clinicopathological characteristics and PDRG1 expression. The variables with p value < 0.1 in univariate Cox regression will be included in further analyzation by multivariate Cox regression. The results were showed in Table 4. The variables that meet this threshold were T stage (p < 0.001), M stage (paired 0.018), Pathologic stage (p < 0.001), Tumor status (p < 0.001), TP53 status (p = 0.069) and PDRG1 (p < 0.001). Furthermore, multivariate Cox regression showed that Tumor status (P = 0.002) and PDRG1 (P = 0.024) were independent prognostic factors in OS of HCC patients. Furthermore, we compared the correlation of PDRG1 expression and OS of different clinicopathological subgroups in HCC patients (Fig. 10–11). It showed that high expression of PDRG1 was correlated with worse OS in T1&T2 stage (HR=1.872, P□0.008), T3 stage (HR□2.541, P□0.004), N0 stage (HR□1.778, P□0.009), M0 stage (HR□2.093, P□0.001). These results suggested that PDRG1 expression level can impact the prognosis in HCC patients with different pathological stages.

To provide clinicians with a quantitative approach to predict the prognosis of HCC patients, a nomogram (Fig. 12) was constructed to integrate PDRG1 and another independent prognostic variable tumor status. In this nomogram based on multivariate Cox analysis, a point scale was used to assign points to these variables. A straight line was drawn upward to determine the points to these variables, and the sum of the points assigned for each variable was rescaled to a range from 0 to 100. The range of available values of PDRG1 was from 0 to 78, it indicated that PDRG1 played an important role in the contribution to the OS of HCC patients. The points of the variables were accumulated and recorded as the total points. A worse prognosis was represented by a higher total number of points on the nomogram. The probability of HCC patient survival at 1, 3 and 5 years was determined by drawing a vertical line from the total point axis straight downward to the outcome axis. OS rate at 1, 3 and 5 years of HCC patients with tumor-free status in high expression of PDRG1 group were 0.86, 0.69, 0.54. The bias-corrected line in the calibration plot was found to be close to the ideal curve (the 45-degree line), which indicated good agreement between the prediction and observation (Fig. 13).

Figure 11. Kaplan-Meier Plotter showed that high expression of PDRG1 was associated with worse Overall Survival of HCC patients in different subgroups of clinicopathological factors. A. T1&T2 stage (HR=1.872, P□0.008); B. T3 stage (HR□2.541, P□0.004); C. N0 stage (HR□1.778, P□0.009); D. M0 stage (HR□2.093, P□0.001).

Figure 13: Calibration plot of the nomogram for predicting the probability of OS at 1, 3, and 5 years. red line: 1-year OS; blue line: 3-year OS; green line: 5-year OS; grey line: ideal line.

Table 4
univariate / multivariate Cox regression analysis on Overall Survival in HCC patients

Characteristics	Total(n)	Univariate analysis		Multivariate analysis	
		HR (95% CI)	P value	HR (95% CI)	P value
T stage (T3&T4 vs. T1&T2)	367	2.540(1.785–3.613)	< 0.001	1.668(0.222–12.539)	0.619
N stage (N1 vs. N0)	256	2.004(0.491–8.181)	0.333		
M stage (M1 vs. M0)	270	4.032(1.267–12.831)	0.018	1.310(0.308–5.577)	0.715
Pathologic stage (Stage III &Stage IV vs. Stage I &Stage II)	346	2.449(1.689–3.549)	< 0.001	1.450(0.194–10.808)	0.717
Residual tumor (R1&R2 vs. R0)	341	1.571(0.795–3.104)	0.194		
Histologic grade (G3&G4 vs. G1&G2)	365	1.120(0.781–1.606)	0.539		
Gender (Male vs. Female)	370	0.816(0.573–1.163)	0.260		
Age (> 60 vs. <=60)	370	1.248(0.880–1.768)	0.214		
Race (White vs. Asian &Black or African American)	358	1.245(0.867–1.789)	0.235		
Weight (> 70 vs. <=70)	343	0.916(0.640–1.312)	0.634		
Height (> = 170 vs. < 170)	338	1.208(0.833–1.753)	0.319		
Adjacent hepatic tissue inflammation (Mild &Severe vs. None)	233	1.228(0.755–1.997)	0.409		
AFP (ng/ml) (> 400 vs. <=400)	277	1.056(0.646–1.727)	0.827		
Albumin(g/dl) (< 3.5 vs. >=3.5)	296	1.085(0.665–1.771)	0.743		
Prothrombin time (< = 4 vs. >4)	293	0.752(0.496–1.140)	0.179		
Child-Pugh grade (B&C vs. A)	238	1.616(0.797–3.275)	0.183		
Fibrosis ishak score (3/4&5/6 vs. 1/2)	137	0.806(0.375–1.737)	0.583		
Vascular invasion (Yes vs. No)	314	1.348(0.890–2.042)	0.159		

Characteristics	Total(n)	Univariate analysis		Multivariate analysis	
		HR (95% CI)	P value	HR (95% CI)	P value
Tumor status	351	2.361(1.620–3.441)	< 0.001	2.189(1.328–3.608)	0.002
TP53 status (Mut vs. WT)	357	1.434(0.972–2.115)	0.069	1.460(0.870–2.451)	0.152
PDRG1 (High vs. Low)	370	1.984(1.391–2.828)	< 0.001	1.747(1.077–2.835)	0.024

Construction And Evaluation Of The Nomogram

we compared PDRG1 expression in patients with HCC and healthy people, and evaluated the discrimination ability of PDRG1 in HCC by receiver operating characteristic (ROC) analysis using pROC package[23]. The computed area under the curve (AUC) value ranging from 0.5 to 1.0 indicates the discrimination ability from 50 to 100%. All statistical tests were two tailed with a statistical significance level set at 0.05 in this study.

To individualize the predicted survival probability for 1 year, 3 years and 5 years, a nomogram was constructed based on the results of the multivariate analysis. The rms R package (version 6.0–1) was used to generate a nomogram that included significant clinical characteristics and calibration plots. Calibration and discrimination are the most commonly used methods for evaluating the performance of models. In this study, the calibration curves were graphically assessed by mapping the nomogram predicted probabilities against the observed rates, and the 45° line represented the best predictive values.

Statistical analysis

All the data were presented as mean ± SD. OS was calculated by the Kaplan Meier method and analyzed with the log-rank test. The univariate and multivariate analyses were calculated based on the Cox regression model. The statistical analysis was performed as appropriate by chi-square test and t-test. The P value of the test was 2-tailed with a level of significance (α) = 0.05. The P-value < 0.05 were considered statistically significant.

Results

Identification of high expression of PDRG1 in HCC tumor tissue

The RNAseq data from TCGA and GTEx in TPM format was downloaded from UCSC XENA, which has been uniformly processed by the Toil process [11]. We compared the expression of PDRG1 in normal samples from GTEx combined with TCGA and HCC samples from TCGA by Wilcoxon rank sum test (Fig. 1A). It was found that PDRG1 showed significantly higher expression in tumor tissues than in normal tissues (P < 0.001). Moreover, we also analyzed the expression of PDRG1 in HCC tumor issues compared with 50 pairs of non-cancerous adjacent tissues using Wilcoxon signed rank test (Fig. 1B). It was found that the expression of

PDRG1 was significantly higher in HCC tumor tissues than non-cancerous adjacent tissues, and the result was statistically significant ($p < 0.001$).

Clinical Characteristics

The data were collected from TCGA on June 2020 and included 371 HCC patients with clinical characteristics and PDRG1 expression data. According to the expression level of PDRG1, the patients were divided into two groups: high expression of PDRG1 and low expression of PDRG1, considering the median was cut-off point. The characteristics of HCC patients including gender, race, age, height, weight, TNM stage, pathologic stage, residual tumor, histologic grade, adjacent hepatic tissue inflammation, Child-Pugh grade, fibrosis ishak score, vascular invasion, tumor status, TP53 status, AFP (ng/ml), albumin (g/dl) and prothrombin time were collected (Table 1). The data were analyzed by chi-square test or t-test. It showed that there were no significant differences in variables including gender ($p = 0.484$), race ($p = 0.644$), age ($p = 0.275$), height ($p = 0.219$), weight ($p = 0.15$), N stage ($p = 0.368$), M stage ($p = 1$), adjacent hepatic tissue inflammation ($p = 0.246$), Child-Pugh grade ($p = 0.65$), tumor status ($p = 0.069$), albumin ($p = 0.559$) and prothrombin time ($p = 0.106$) in groups with high/low expression of PDRG1. There were significant differences in variables including T stage ($p = 0.006$), pathologic stage ($p = 0.018$), residual tumor ($p = 0.024$), histologic grade ($p < 0.001$), fibrosis ishak score ($p = 0.019$), vascular invasion ($p = 0.008$), TP53 status ($p < 0.001$), AFP ($p < 0.001$).

Then we used Kruskal-Wallis rank sum test to compare the relation between expression of PDRG1 and clinicopathological features in HCC patients (Fig. 2). It showed that the expression of PDRG1 in HCC patients were significantly associated with T stage ($p = 0.006$), pathologic stage ($p = 0.012$), residual tumor ($p = 0.121$), histologic grade ($p < 0.001$), AFP ($p < 0.001$), fibrosis ishak score ($p = 0.007$), vascular invasion ($p = 0.035$), TP53 status ($p < 0.001$). Moreover, we used Logistics regression to analyze the relationship between clinicopathological features of HCC patients and PDRG1 high/low 2 classification (Table 2). We found that PDRG1 expression was significantly associated with T stage ($p = 0.049$), residual tumor ($p = 0.047$), histologic grade ($p < 0.001$), vascular invasion ($p = 0.006$), TP53 status ($p < 0.001$), and AFP ($p < 0.001$).

Table 1
Clinical Characteristics

Characteristics	level	Low expression of PDRG1	High expression of PDRG1	p	Test*
T stage (%)	T1	107(58.5%)	74(40.0%)	0.006	
	T2	38(20.8%)	56(30.3%)		
	T3	33(18.0%)	47(25.4%)		
	T4	5(2.7%)	8(4.3%)		
N stage (%)	N0	128(99.2%)	124(97.6%)	0.368	exact
	N1	1(0.8%)	3(2.4%)		
M stage (%)	M0	136(98.6%)	130(98.5%)	1.000	exact
	M1	2(1.4%)	2(1.5%)		
Pathologic stage (%)	Stage I	99(57.2%)	72(41.4%)	0.018	exact
	Stage II	37(21.4%)	49(28.2%)		
	Stage III	34(19.7%)	51(29.3%)		
	Stage IV	3(1.7%)	2(1.1%)		
Residual tumor (%)	R0	171(97.2%)	153(92.2%)	0.024	exact
	R1	4(2.3%)	13(7.8%)		
	R2	1(0.6%)	0(0.0%)		
Histologic grade (%)	G1	39(21.2%)	16(8.8%)	< 0.001	
	G2	94(51.1%)	83(45.6%)		
	G3	49(26.6%)	73(40.1%)		
	G4	2(1.1%)	10(5.5%)		
Gender (%)	Female	57(30.6%)	64(34.6%)	0.484	
	Male	129(69.4%)	121(65.4%)		
Race (%)	Asian	74(41.6%)	84(46.4%)	0.644	exact
	Black or African American	9(5.1%)	8(4.4%)		
	White	95(53.4%)	89(49.2%)		

* classification variables use chi-square test for statistical analysis, and “exact” indicates that the statistical method is Fisher's exact test. Numerical variables use t-test for statistical analysis, "nonnorm" is represented as a non-normal distribution, and Wilcoxon rank sum test is used for statistical analysis.

Characteristics	level	Low expression of PDRG1	High expression of PDRG1	p	Test*
Adjacent hepatic tissue inflammation (%)	Mild	50(37.6%)	49(48.5%)	0.246	
	None	72(54.1%)	45(44.6%)		
	Severe	11(8.3%)	7(6.9%)		
Child-Pugh grade (%)	A	109(89.3%)	108(92.3%)	0.650	exact
	B	12(9.8%)	9(7.7%)		
	C	1(0.8%)	0(0.0%)		
Fibrosis ishak score (%)	0	49(40.5%)	25(27.5%)	0.019	
	1/2	14(11.6%)	17(18.7%)		
	3/4	10(8.3%)	18(19.8%)		
	5/6	48(39.7%)	31(34.1%)		
Vascular invasion (%)	No	117(72.7%)	89(57.8%)	0.008	
	Yes	44(27.3%)	65(42.2%)		
Tumor status (%)	Tumor free	110(62.1%)	91(52.0%)	0.069	
	With tumor	67(37.9%)	84(48.0%)		
TP53 status (%)	Mut	33(18.2%)	69(39.0%)	< 0.001	
	WT	148(81.8%)	108(61.0%)		
Age (median [IQR])		60.0[51.0, 68.0]	61.5[52.0, 69.0]	0.275	nonnorm
Height (median [IQR])		168.0[160.5, 175.0]	167.0[161.8, 172.0]	0.219	nonnorm
Weight (median [IQR])		71.5[59.0, 85.0]	68.5[59.0, 80.0]	0.150	nonnorm
AFP (ng/ml) (median [IQR])		8.0[3.0, 47.8]	30.0[6.0, 2212.5]	< 0.001	nonnorm
Albumin(g/dl) (median [IQR])		4.0[3.4, 4.3]	4.0[3.5, 4.3]	0.559	nonnorm
Prothrombin time (median [IQR])		1.1[1.0, 9.8]	1.1[1.0, 8.7]	0.106	nonnorm

* classification variables use chi-square test for statistical analysis, and “exact” indicates that the statistical method is Fisher's exact test. Numerical variables use t-test for statistical analysis, "nonnorm" is represented as a non-normal distribution, and Wilcoxon rank sum test is used for statistical analysis.

Table 2
Logistics regression analyzed the relationship between clinicopathological features of HCC patients and two classifications of high / low PDRG1 expression

Characteristics	Odds Ratio in PDRG1 expression	Odds Ratio (OR)	P value
T stage (T3&T4 vs. T1&T2)	368	1.61(1.01–2.61)	0.049
N stage (N1 vs. N0)	256	3.10(0.39–63.07)	0.330
M stage (M1 vs. M0)	270	1.05(0.12–8.82)	0.964
Pathologic stage (Stage III & Stage IV vs. Stage I & Stage II)	347	1.61(0.99–2.63)	0.055
Residual tumor (R1&R2 vs. R0)	342	2.91(1.07–9.23)	0.047
Histologic grade (G3&G4 vs. G1&G2)	366	2.19(1.42–3.39)	< 0.001
Adjacent hepatic tissue inflammation (Mild & Severe vs. None)	234	1.47(0.87–2.48)	0.147
AFP (ng/ml) (> 400 vs. <=400)	278	3.26(1.82-6.00)	< 0.001
Child-Pugh grade (B&C vs. A)	239	0.70(0.28–1.69)	0.430
Fibrosis ishak score (3/4&5/6 vs. 1/2)	138	0.70(0.31–1.55)	0.376
Vascular invasion (Yes vs. No)	315	1.94(1.22–3.13)	0.006
Tumor status (With tumor vs. Tumor free)	352	1.52(0.99–2.32)	0.055
TP53 status (Mut vs. WT)	358	2.87(1.78–4.69)	< 0.001

Discussion

The cloning and characterization of PDRG was first reported by X Luo et al [2]on 2003. In normal human tissues, PDRG exhibited maximal expression in the testis and minimal levels in the liver. PDRG mRNA would be upregulated by genotoxic stress containing ultraviolet radiation and the transcription factor Oct-1 via Oct-1 binding element located at -689/-683[2, 24], but it would be downregulated by tumor suppressor p53 though directly binding to p53 binding element located at -240/-214[25–27] or p53 transcriptional repressor element (TRE, located at -854/-834[28]) such as p21, PIG-3, PTGF-b1. PDRG1 is a nucleocytoplasmic protein of the R2TP/prefoldin-like complex that has been found as part of different multiprotein complexes[29, 30]. Previous studies on PPI involving PDRG1 identified that the PDRG1 protein has been found as part of the RNA

polymerase complex[29], and the URI/prefoldin complex involved in nutrient signaling[30–32]. It may have a role in chromatin remodeling, splicing and apoptosis[3, 33–35]. Moreover, studies also showed that PDRG1 was involved a variety of cellular physiological activities, such as apoptosis, DNA damage repair, cell cycle regulation and promoting programmed cell death after growth factor starvation[2]. Zhang W et.al found that PDRG1 plays an important role in diapause termination and cell cycle regulation in early embryonic development of Artemia sinica[36]. The expression of PDRG1 was upregulated in several tumors including colon (82%), rectum (78%), ovary (71%), lung (70%), stomach (68%), breast (63%) and uterus (62%) when compared with their matched normal tissues[3]. It suggested that PDRG1 may be a high-value novel tumor marker which could play an important role in cancer development and/or progression. Recent study indicated that miR-214 could exert tumor-suppressive effects in bladder cancer by directly down-regulating oncogene PDRG1[8]. Correlation of elevated PDRG1 and GLUT1 expression with poor pathological response has been reported in residual rectal cancer cells after pre-operative chemotherapy[7]. Moreover, it was reported that Oleuropein enhances radiation sensitivity of nasopharyngeal carcinoma by downregulating PDRG1 through HIF1α-repressed microRNA-519d[37]. But there were fewer researches focused on the expression of PDRG1 in HCC patients. In this study, we demonstrated that the expression of PDRG1 was higher in HCC tissues in contrast to normal liver tissues, the result was consistent with previous studies on PDRG1 in other tumors. High expression of PDRG1 in HCC patients was significantly correlated with adverse clinicopathological features, such as advanced T stage, residual tumor, histologic grade and vascular invasion. These results suggested that PDRG1 may play a role in the development of HCC. In order to investigate the role of PDRG1 in hepatocellular carcinoma, we performed GO analyses on PDRG1 co-expressed genes and found that PDRG1 participated in biological processes including pattern specification process, skeletal system development, multicellular organismal homeostasis, reproductive structure development, epithelial cell differentiation, sensory organ development, metanephros development, gonadal mesoderm development, mesenchyme development, and negative regulation of cell differentiation. In order to explore the underlying molecular mechanisms of PDRG1 in HCC patients, we conduct GSEA comparing the high/low expression of PDRG1 in HCC patients, and we found that PDRG1 participated in the DNA repair, DNA replication and cell cycle, the result was consistent with previous studies. PDRG1 protein was found as an interaction target for the catalytic subunits of methionine adenosyltransferases, indicated that it could downregulated the S-adenosylmethionine synthesis, resulting in reduced DNA methylation levels[9]. Previous study had indicated that S-adenosylmethionine and Methylthioadenosine were proapoptotic in human Hepatoma Cells (HepG2 cell)[38]. Increased expression of PDRG1 have been associated with several types of tumors that concomitantly show global DNA hypomethylation, highlighting the importance of this interaction as one of the putative underlying causes for cell transformation[39]. Moreover, PDRG1 played a valuable role in controlling cell growth regulation involved in apoptosis and cell cycle regulation via interaction with proteins such as PDCD7, MAP1S, CIZ[3]. PDRG1 could promote radioresistance involved the ATM/p53 signaling pathway in lung cancer[4]. Specific PDRG1 gene silencing may inhibit the growth and metastasis of gastric cancer cells through the activation of ATM/p53 pathway[6],so we speculate that it could play a similar role in hepatocellular carcinoma.

According to degree centrality and molecular module analysis of differentially expressed proteins in the PPI network, the crucial proteins including SST, CALCA, GLP1R, AFP, FOXG1, GAGE2A, DLX2, CDX2, SIX3, FOXG1, NTS were identified. Here, we talked about 3 proteins including SST, CALCA, FOXG1. Somatostatin (SST) acts

as an inhibitory peptide of various secretory and proliferative processes. SST and its analogues were found involving growth arrest and apoptotic actions mediated directly by SSTR present on tumor cells and indirectly via SSTR present on a nontumor cell target [40–42]. LincRNA-CALCA was reported as one of the most downregulated lincRNA in cell line HCCLYM-H2(H2), which showed stable and high metastatic potential specific to the lymph nodes[43]. Forkhead box G1 (FOXG1) is a member of the Fox transcription factor family involved in regulation of many cancers. It was reported that FOXG1 played a key role in mediating cancer cell metastasis through the Wnt/β-catenin pathway in HCC cells and predicted HCC prognosis after surgery[44].

Tumor-associated immune response plays a critical role in cancer pathogenesis. Here, we performed Spearman correlation to show the association between the expression level of PDRG1 and immune cell infiltration level quantified by ssGSEA in the HCC tumor microenvironment. The result indicated that high expression of PDRG1 was significantly correlated with Th2 cells level in HCC patients. Significantly increased of Th2 response would change the Th1/Th2 balance, induced an adverse immunologic effect on HCC prognosis. However, the specific molecular mechanism of PDRG1 and immune cell infiltration in HCC is still unclear, which needs further experimental confirmation.

Moreover, we demonstrated that Tumor status and PDRG1 were independent prognostic factors in OS of HCC patients. Therefore, we propose a comprehensive assessment that combines Tumor status and PDRG1. The calibration curve showed satisfactory agreement between the observed values and the predicted values for 1-, 3-, and 5-year OS. In summary, these finding suggested that the nomogram base on PDRG1 and tumor status was a well model for predicting short-term or long-term survival in HCC patients.

In addition, several limitations should be mentioned. Firstly, this study lacked further experimental verification of the effects on the expression and functions of PDRG1 in HCC. Secondly, the specific molecular mechanism of PDRG1 in the development and progression in HCC is still unclear, which needs further experimental confirmation. Thirdly, our studies were only based on single-gene PDRG1, and it can’t be measured in serum. Whether it can improve the diagnostic and prognostic efficacy of hepatocellular carcinoma when analyze PDRG1 combined with other genes, it need be further researched.

Conclusion

Our study demonstrated the potential significance of PDRG1 expression in the diagnosis and prognosis of HCC and further explored the function in HCC. Further study is still needed in order to confirm these results. The underlying mechanism revealed by these results provides a basis for PDRG1 as a new molecular target for the prevention and treatment of HCC.

Abbreviations

PDRG1
p53 and DNA damage-regulated gene 1; HCC:Hepatocellular carcinoma; Gene set enrichment analysis (GSEA); TCGA:The Cancer Genome Atlas; PPI:protein-protein interactions; GEO:Gene Expression Omnibus; FDR:False discovery rate; ROC:receiver operating characteristic; AUC:area under the curve; SD:standard deviation.

Declarations

Acknowledgements

None.

Authors’ contributions

JYL designed the study, performed the research, and wrote the paper.

XD and YYW performed research and analyzed data.

ZHC performed research and checked the data.

HWP helped performed research and checked the data.

KZ designed the study and analyzed data.

The authors read and approved the final manuscript.

Funding

This work was supported by College-level Project Fund of the people's Hospital affiliated to Jiangsu University (grant number Y2019014).

Availability of data and materials

The datasets used during the present study are available from the corresponding author on reasonable request.

Ethics approval and consent to participate

All analyses were based on previous published studies, thus no ethical approval and patient consent are required.

Consent for publication

None.

Competing interests

The authors declare that they have no competing interests.

Author details

1. Department of General Surgery, Affiliated People's Hospital of Jiangsu University, Jiangsu University, Zhenjiang, Jiangsu, 212002, P. R. China.

2. Department of Thoracic Surgery, Affiliated People's Hospital of Jiangsu University, Jiangsu University, Zhenjiang, Jiangsu, 212002, P. R. China.

3. Department of Neurology, Affiliated People's Hospital of Jiangsu University, Jiangsu University, Zhenjiang, Jiangsu, 212002, P. R. China.

References

References

1. Lafaro KJ, Demirjian AN, Pawlik TM. Epidemiology of hepatocellular carcinoma. Surg Oncol Clin N Am. 2015;24(1):1–17. https://doi.org/10.1016/j.soc.2014.09.001.
2. Luo X, Huang Y, Sheikh MS. Cloning and characterization of a novel gene PDRG that is differentially regulated by p53 and ultraviolet radiation. Oncogene. 2003;22(46):7247–57. https://doi.org/10.1038/sj.onc.1207010.
3. Jiang L, Luo X, Shi J, Sun H, Sun Q, Sheikh MS, Huang Y. PDRG1, a novel tumor marker for multiple malignancies that is selectively regulated by genotoxic stress. Cancer Biol Ther. 2011;11(6):567–73. https://doi.org/10.4161/cbt.11.6.14412.
4. Tao Z, Chen S, Mao G, Xia H, Huang H, Ma H. The PDRG1 is an oncogene in lung cancer cells, promoting radioresistance via the ATM-P53 signaling pathway. Biomed Pharmacother. 2016;83:1471–7. https://doi.org/10.1016/j.biopha.2016.08.034.
5. Al-Joudi FS, Iskandar ZA, Rusli J. The expression of p53 in invasive ductal carcinoma of the breast: a study in the North-East States of Malaysia. Med J Malay. 2008;63(2):96–9.
6. Zhang YJ, Li JQ, Li HZ, Song H, Wei CS, Zhang SQ. PDRG1 gene silencing contributes to inhibit the growth and induce apoptosis of gastric cancer cells. Pathol Res Pract. 2019;215(10):152567. https://doi.org/10.1016/j.prp.2019.152567.
7. Saigusa S, Tanaka K, Toiyama Y, Matsushita K, Kawamura M, Okugawa Y, Hiro J, Inoue Y, Uchida K, Mohri Y, et al. Gene expression profiles of tumor regression grade in locally advanced rectal cancer after neoadjuvant chemoradiotherapy. Oncol Rep. 2012;28(3):855–61. https://doi.org/10.3892/or.2012.1863.
8. Wang J, Zhang X, Wang L, Yang Y, Dong Z, Wang H, Du L, Wang C. MicroRNA-214 suppresses oncogenesis and exerts impact on prognosis by targeting PDRG1 in bladder cancer. PLoS One. 2015;10(2):e0118086. https://doi.org/10.1371/journal.pone.0118086.
9. Pérez C, Pérez-Zúñiga FJ, Garrido F, Reytor E, Portillo F, Pajares MA. The Oncogene PDRG1 Is an Interaction Target of Methionine Adenosyltransferases. PLoS One. 2016;11(8):e0161672. https://doi.org/10.1371/journal.pone.0161672.
10. Li CY, Liang GY, Yao WZ, Sui J, Shen X, Zhang YQ, Peng H, Hong WW, Ye YC, Zhang ZY, et al. Identification and functional characterization of microRNAs reveal a potential role in gastric cancer progression. Clinical translational oncology: official publication of the Federation of Spanish Oncology Societies of the National Cancer Institute of Mexico. 2017;19(2):162–72. https://doi.org/10.1007/s12094-016-1516-y.
11. Vivian J, Rao AA, Nothaft FA, Ketchum C, Armstrong J, Novak A, Pfeil J, Narkizian J, Deran AD, Musselman-Brown A, et al. Toil enables reproducible, open source, big biomedical data analyses. Nature biotechnology. 2017;35(4):314–6. https://doi.org/10.1038/nbt.3772.

12. Love MI, Huber W, Anders S. Moderated estimation of fold change and dispersion for RNA-seq data with DESeq2. Genome biology. 2014;15(12):550. https://doi.org/10.1186/s13059-014-0550-8.
13. Zhou Y, Zhou B, Pache L, Chang M, Khodabakhshi AH, Tanaseichuk O, Benner C, Chanda SK. Metascape provides a biologist-oriented resource for the analysis of systems-level datasets. Nat Commun. 2019;10(1):1523. https://doi.org/10.1038/s41467-019-09234-6.
14. Subramanian A, Tamayo P, Mootha VK, Mukherjee S, Ebert BL, Gillette MA, Paulovich A, Pomeroy SL, Golub TR, Lander ES, et al. Gene set enrichment analysis: a knowledge-based approach for interpreting genome-wide expression profiles. Proc Natl Acad Sci USA. 2005;102(43):15545–50. https://doi.org/10.1073/pnas.0506580102.
15. Yu G, Wang LG, Han Y, He QY. clusterProfiler: an R package for comparing biological themes among gene clusters. Omics: a journal of integrative biology. 2012;16(5):284–7. https://doi.org/10.1089/omi.2011.0118.
16. Szklarczyk D, Gable AL, Lyon D, Junge A, Wyder S, Huerta-Cepas J, Simonovic M, Doncheva NT, Morris JH, Bork P, et al. STRING v11: protein-protein association networks with increased coverage, supporting functional discovery in genome-wide experimental datasets. Nucleic acids research. 2019;47(D1):D607-d613. https://doi.org/10.1093/nar/gky1131.
17. Shannon P, Markiel A, Ozier O, Baliga NS, Wang JT, Ramage D, Amin N, Schwikowski B, Ideker T. Cytoscape: a software environment for integrated models of biomolecular interaction networks. Genome research. 2003;13(11):2498–504. https://doi.org/10.1101/gr.1239303.
18. Smoot ME, Ono K, Ruscheinski J, Wang PL, Ideker T. Cytoscape 2.8: new features for data integration and network visualization. Bioinformatics. 2011;27(3):431–2. https://doi.org/10.1093/bioinformatics/btq675.
19. Bandettini WP, Kellman P, Mancini C, Booker OJ, Vasu S, Leung SW, Wilson JR, Shanbhag SM, Chen MY, Arai AE. MultiContrast Delayed Enhancement (MCODE) improves detection of subendocardial myocardial infarction by late gadolinium enhancement cardiovascular magnetic resonance: a clinical validation study. Journal of cardiovascular magnetic resonance: official journal of the Society for Cardiovascular Magnetic Resonance. 2012;14(1):83. https://doi.org/10.1186/1532-429x-14-83.
20. Tang Y, Li M, Wang J, Pan Y, Wu FX. CytoNCA: a cytoscape plugin for centrality analysis and evaluation of protein interaction networks. Bio Syst. 2015;127:67–72. https://doi.org/10.1016/j.biosystems.2014.11.005.
21. Hänzelmann S, Castelo R, Guinney J. GSVA: gene set variation analysis for microarray and RNA-seq data. BMC Bioinform. 2013;14:7. https://doi.org/10.1186/1471-2105-14-7.
22. Bindea G, Mlecnik B, Tosolini M, Kirilovsky A, Waldner M, Obenauf AC, Angell H, Fredriksen T, Lafontaine L, Berger A, et al. Spatiotemporal dynamics of intratumoral immune cells reveal the immune landscape in human cancer. Immunity. 2013;39(4):782–95. https://doi.org/10.1016/j.immuni.2013.10.003.
23. Robin X, Turck N, Hainard A, Tiberti N, Lisacek F, Sanchez JC, Müller M. pROC: an open-source package for R and S + to analyze and compare ROC curves. BMC Bioinform. 2011;12:77. https://doi.org/10.1186/1471-2105-12-77.
24. Latchman DS: **POU family transcription factors in the nervous system**. *J Cell Physiol* 1999, **179**(2):126–133. https://doi.org/10.1002/(sici)1097-4652(199905)179:2<126::Aid-jcp2>3.0.Co;2-m.

25. Johnson RA, Ince TA, Scotto KW. Transcriptional repression by p53 through direct binding to a novel DNA element. J Biol Chem. 2001;276(29):27716–20. https://doi.org/10.1074/jbc.C100121200.
26. Resnick-Silverman L, St Clair S, Maurer M, Zhao K, Manfredi JJ: **Identification of a novel class of genomic DNA-binding sites suggests a mechanism for selectivity in target gene activation by the tumor suppressor protein p53**. *Genes & development* 1998, **12**(14):2102–2107. https://doi.org/10.1101/gad.12.14.2102.
27. el-Deiry WS, Kern SE, Pietenpol JA, Kinzler KW, Vogelstein B: **Definition of a consensus binding site for p53**. *Nature genetics* 1992, **1**(1):45–49. https://doi.org/10.1038/ng0492-45.
28. Wong J, Li PX, Klamut HJ. A novel p53 transcriptional repressor element (p53TRE) and the asymmetrical contribution of two p53 binding sites modulate the response of the placental transforming growth factor-beta promoter to p53. J Biol Chem. 2002;277(29):26699–707. https://doi.org/10.1074/jbc.M203020200.
29. Boulon S, Pradet-Balade B, Verheggen C, Molle D, Boireau S, Georgieva M, Azzag K, Robert MC, Ahmad Y, Neel H, et al. HSP90 and its R2TP/Prefoldin-like cochaperone are involved in the cytoplasmic assembly of RNA polymerase II. Molecular cell. 2010;39(6):912–24. https://doi.org/10.1016/j.molcel.2010.08.023.
30. Mita P, Savas JN, Ha S, Djouder N, Yates JR 3rd, Logan SK. Analysis of URI nuclear interaction with RPB5 and components of the R2TP/prefoldin-like complex. PLoS One. 2013;8(5):e63879. https://doi.org/10.1371/journal.pone.0063879.
31. Sardiu ME, Cai Y, Jin J, Swanson SK, Conaway RC, Conaway JW, Florens L, Washburn MP. Probabilistic assembly of human protein interaction networks from label-free quantitative proteomics. Proc Natl Acad Sci USA. 2008;105(5):1454–9. https://doi.org/10.1073/pnas.0706983105.
32. Sutter BM, Wu X, Laxman S, Tu BP. Methionine inhibits autophagy and promotes growth by inducing the SAM-responsive methylation of PP2A. Cell. 2013;154(2):403–15. https://doi.org/10.1016/j.cell.2013.06.041.
33. Ruhl DD, Jin J, Cai Y, Swanson S, Florens L, Washburn MP, Conaway RC, Conaway JW, Chrivia JC. Purification of a human SRCAP complex that remodels chromatin by incorporating the histone variant H2A.Z into nucleosomes. Biochemistry. 2006;45(17):5671–7. https://doi.org/10.1021/bi060043d.
34. Jin J, Cai Y, Yao T, Gottschalk AJ, Florens L, Swanson SK, Gutiérrez JL, Coleman MK, Workman JL, Mushegian A, et al. A mammalian chromatin remodeling complex with similarities to the yeast INO80 complex. J Biol Chem. 2005;280(50):41207–12. https://doi.org/10.1074/jbc.M509128200.
35. Will CL, Schneider C, Hossbach M, Urlaub H, Rauhut R, Elbashir S, Tuschl T, Lührmann R: **The human 18S U11/U12 snRNP contains a set of novel proteins not found in the U2-dependent spliceosome**. *RNA (New York, NY)* 2004, **10**(6):929–941. https://doi.org/10.1261/rna.7320604.
36. Zhang W, Yao F, Zhang H, Li N, Zou X, Sui L, Hou L. The Potential Roles of the Apoptosis-Related Protein PDRG1 in Diapause Embryo Restarting of Artemia sinica. Int J Mol Sci 2018, 19(1). https://doi.org/10.3390/ijms19010126.
37. Xu T, Xiao D. Oleuropein enhances radiation sensitivity of nasopharyngeal carcinoma by downregulating PDRG1 through HIF1alpha-repressed microRNA-519d. J Exp Clin Cancer Res. 2017;36(1):3. https://doi.org/10.1186/s13046-016-0480-2.
38. Ansorena E, García-Trevijano ER, Martínez-Chantar ML, Huang ZZ, Chen L, Mato JM, Iraburu M, Lu SC, Avila MA. S-adenosylmethionine and methylthioadenosine are antiapoptotic in cultured rat hepatocytes

but proapoptotic in human hepatoma cells. Hepatology. 2002;35(2):274–80. https://doi.org/10.1053/jhep.2002.30419.

39. Pajares M. PDRG1at the interface between intermediary metabolism and oncogenesis. World Journal of Biological Chemistry. 2017;8(4):175–86. https://doi.org/10.4331/wjbc.v8.i4.175.
40. Patel YC. Somatostatin and its receptor family. Front Neuroendocr. 1999;20(3):157–98. https://doi.org/10.1006/frne.1999.0183.
41. Lamberts SW, Reubi JC, Krenning EP. The role of somatostatin analogs in the control of tumor growth. Seminars in oncology. 1994;21(5 Suppl 13):61–4.
42. Lamberts SW, de Herder WW, Hofland LJ. Somatostatin analogs in the diagnosis and treatment of cancer. Trends Endocrinol Metab. 2002;13(10):451–7. https://doi.org/10.1016/s1043-2760(02)00667-7.
43. Fang TT, Sun XJ, Chen J, Zhao Y, Sun RX, Ren N, Liu BB. Long non-coding RNAs are differentially expressed in hepatocellular carcinoma cell lines with differing metastatic potential. Asian Pac J Cancer Prev. 2014;15(23):10513–24. https://doi.org/10.7314/apjcp.2014.15.23.10513.
44. Zheng X, Lin J, Wu H, Mo Z, Lian Y, Wang P, Hu Z, Gao Z, Peng L, Xie C. Forkhead box (FOX) G1 promotes hepatocellular carcinoma epithelial-Mesenchymal transition by activating Wnt signal through forming T-cell factor-4/Beta-catenin/FOXG1 complex. J Exp Clin Cancer Res. 2019;38(1):475. https://doi.org/10.1186/s13046-019-1433-3.

Figures

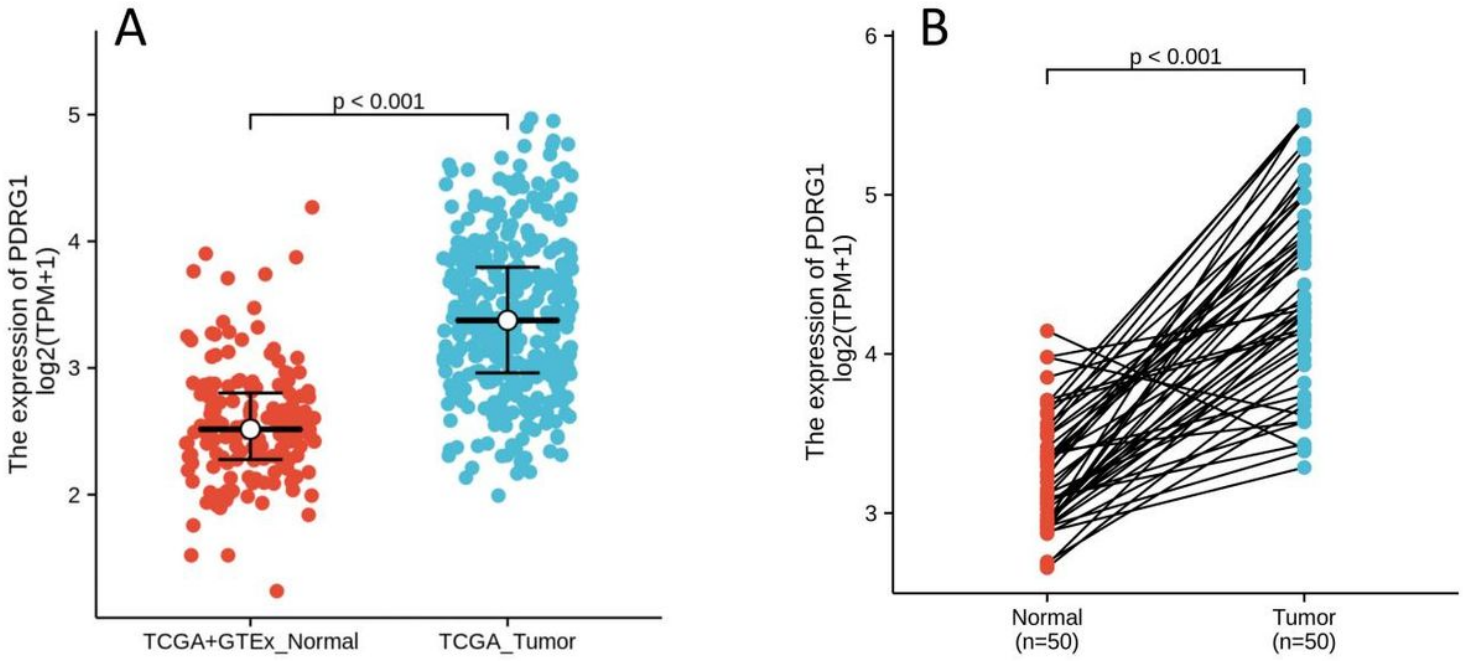

Figure 1

(A) PDRG1 showed significantly higher expression in cancer tissues than in normal tissues (P <0.001). (B) PDRG1 was prominently overexpressed in HCC (P <0.001) compared with 50 pairs non-cancerous adjacent tissue using Wilcoxon singed rank test (P <0.001).

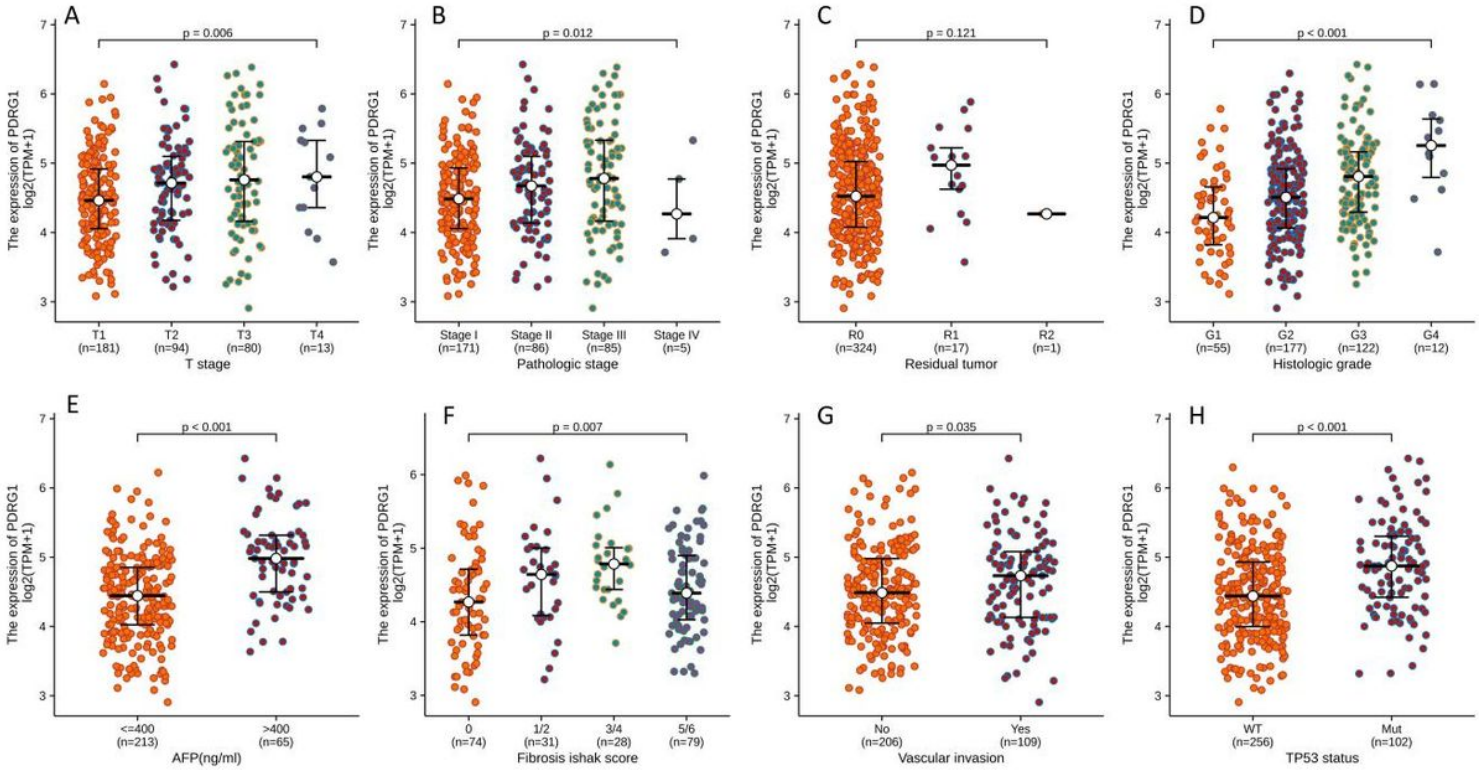

Figure 2

Correlation between PDRG1 expression and clinicopathological features in HCC patients was analyzed by Kruskal-Wallis rank sum test. A: T stage (p=0.006); B: pathologic stage (p=0.012); C: residual tumor (p=0.121); D: histologic grade (p<0.001); E: AFP (p<0.001); F: fibrosis ishak score (p=0.007); G: vascular invasion (p=0.035); H: TP53 status (p<0.001).

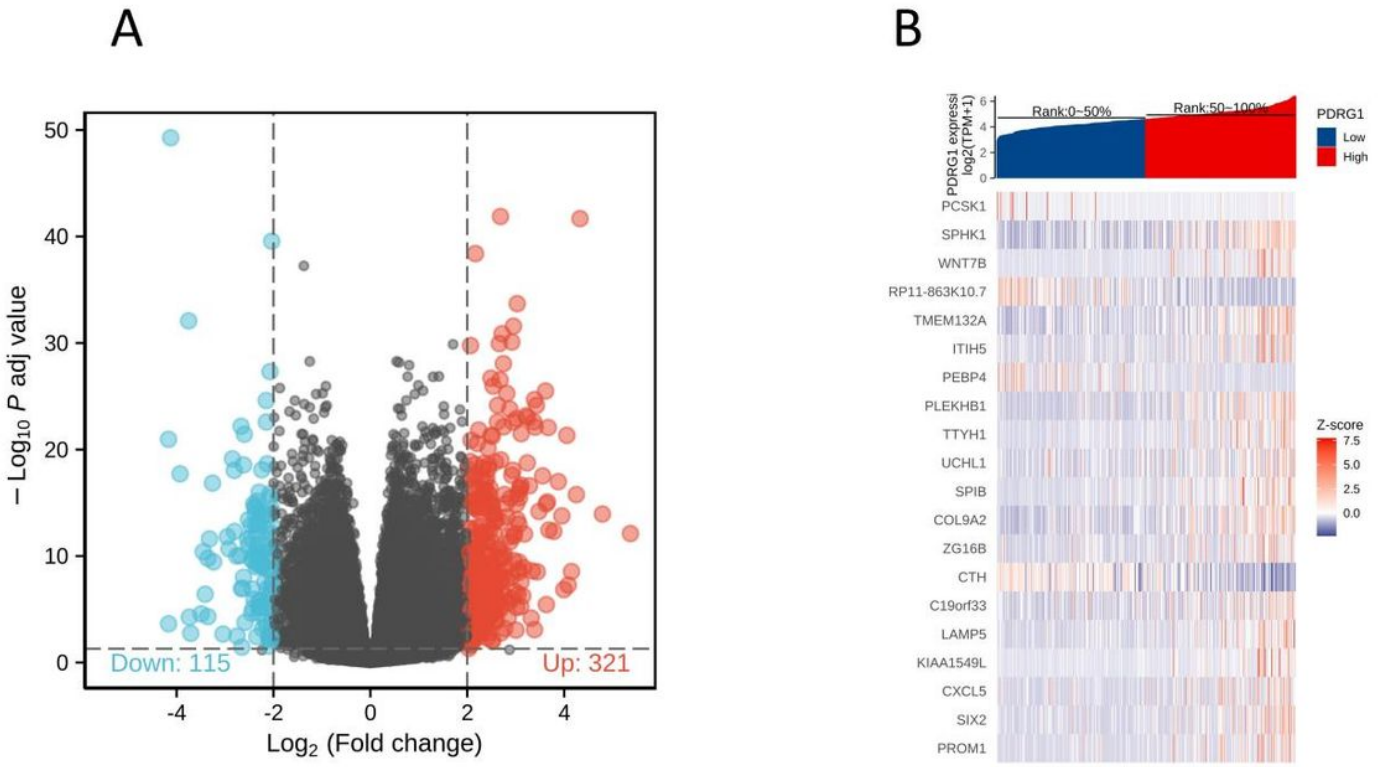

Figure 3

(A) volcano plot of DEGs. (B) heatmap of top 20 DEGs

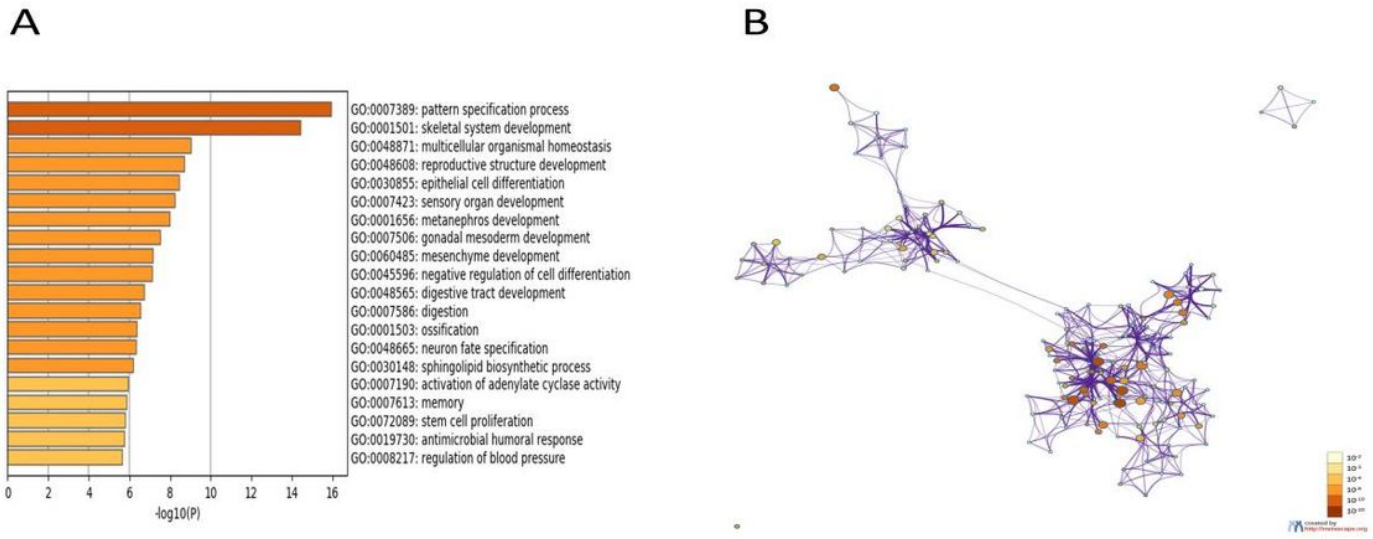

Figure 4

(A) Bar graph of enriched terms across input gene lists, colored by p-values. (B) Network of enriched terms: colored by p-value, where terms containing more genes tend to have a more significant p-value.

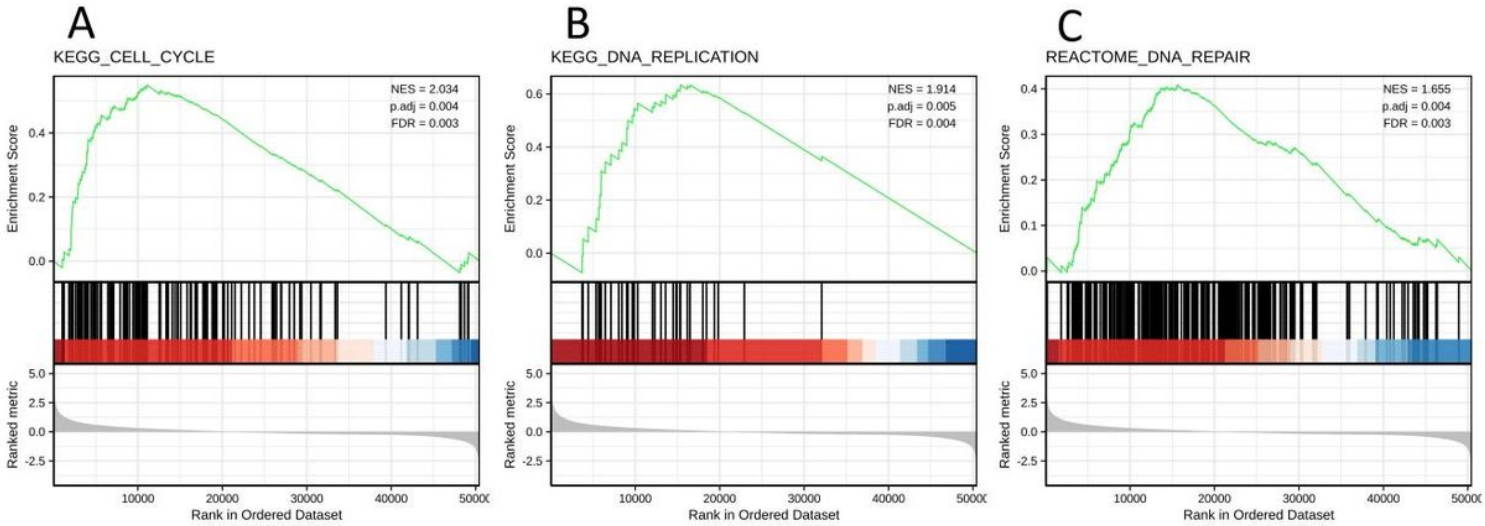

Figure 5

Enrichment plots from the gene set enrichment analysis（GSEA）. The reference gene set is h.all.v7.0.symbols.gmt [Hallmarks]. (A) KEGG_CELL_CYCLE, NES=2.034, p. adj=0.004, FDR=0.003. (B) KEGG_DNA_REPLICATION, NES=1.914, p. adj=0.005, FDR=0.004. (C) REACTOME_DNA_REPAIR, NES=1.655, p. adj=0.004, FDR=0.003. The results suggest that the dataset is significantly enriched in the left red (high PDRG1 expression group). NES, normalized ES; p. adj, adjust p value; FDR, false discovery rate.

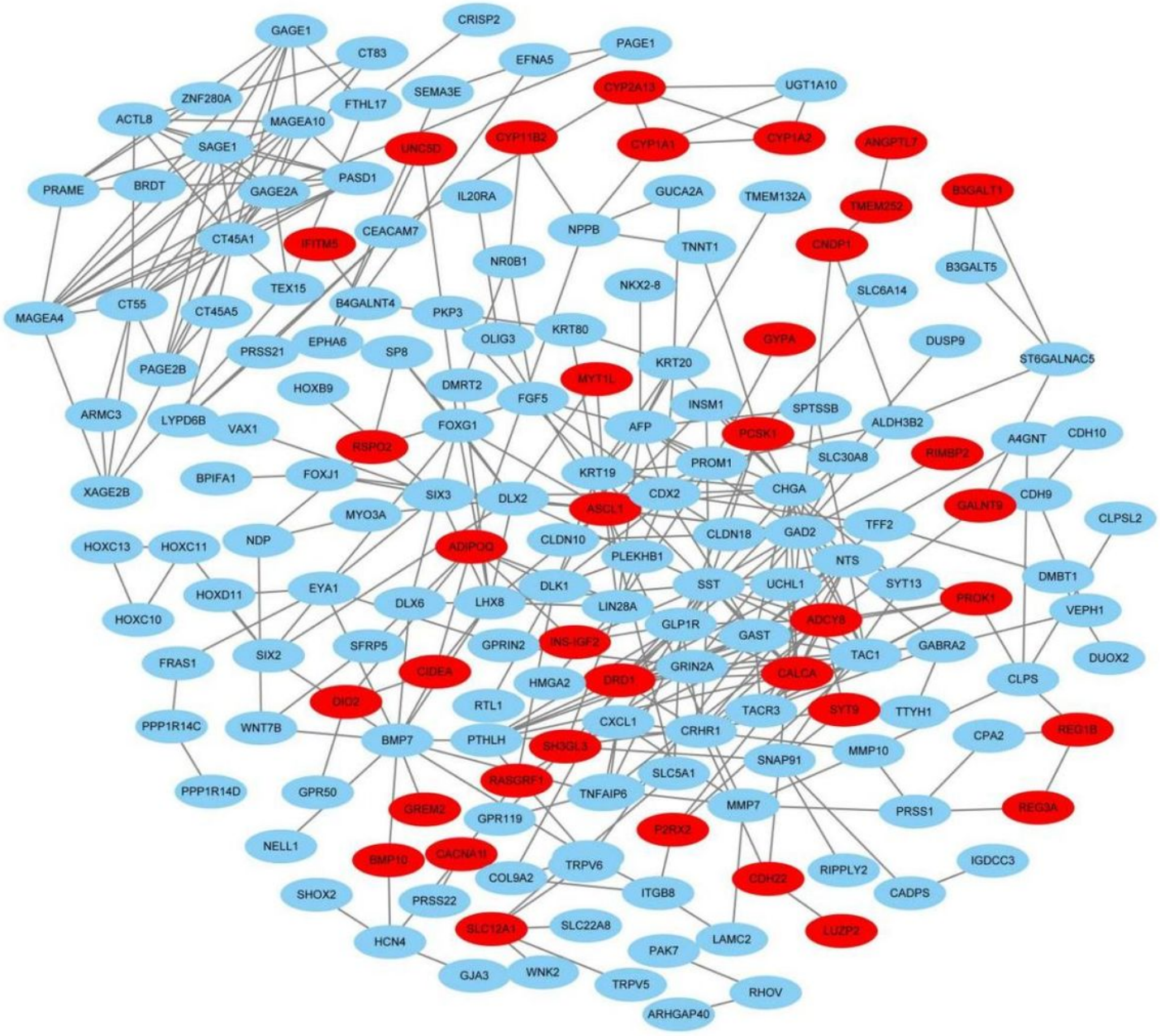

Figure 6

PPI network of DEGs was constructed using Cytoscape including 177 nodes and 367 edges. Downregulated genes are marked in dark red; Upregulated genes are marked in light blue.

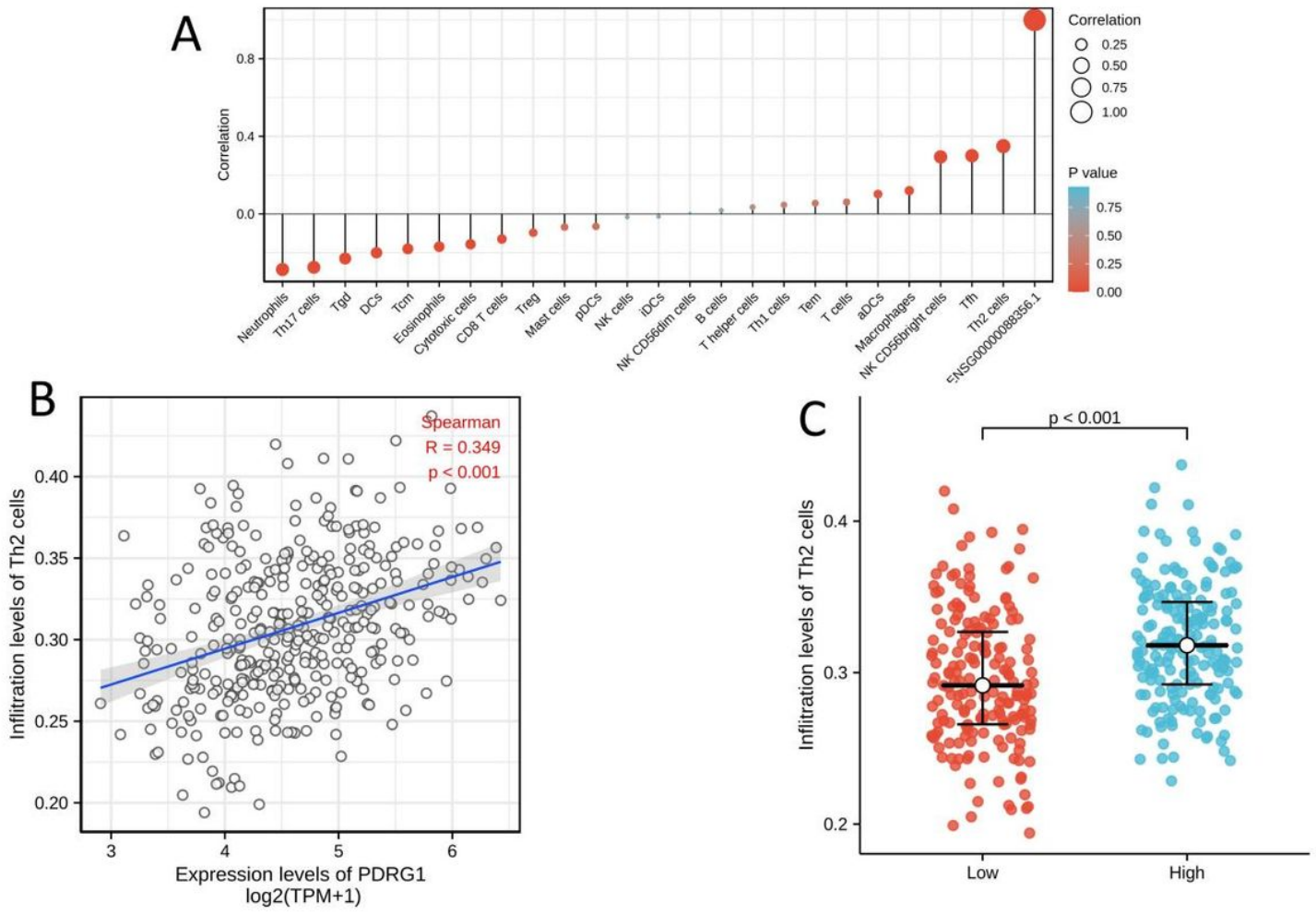

Figure 7

The expression level of PDRG1 was associated with the immune infiltration in the tumor microenvironment. (A) Correlation between the relative abundances of 24 immune cells and PDRG1 expression level. The size of dots shows the correlation coefficient r of spearman. The color shows the P value. The threshold of P value was 1, and threshold of the correlation coefficient was 0. DCs, Dendritic cells; aDCs, activated DCs; iDCs, immature DCs; Th, helper T cells; Treg, Regulatory T cells; T regular; Tgd, T gamma delta; Tcm, T central memory; Tem, T effector memory; Tfh, T follicular helper. (B) Correlation between the expression level of PDRG1 and infiltration levels of Th2 cells. The correlation coefficient R was 0.349 ($P < 0.001$). (C) The difference of Th2 cells infiltration level between PDRG1 high and low expression groups was analyzed by Wilcoxon rank sum test statistical method, and the result was statistically significant ($p < 0.001$).

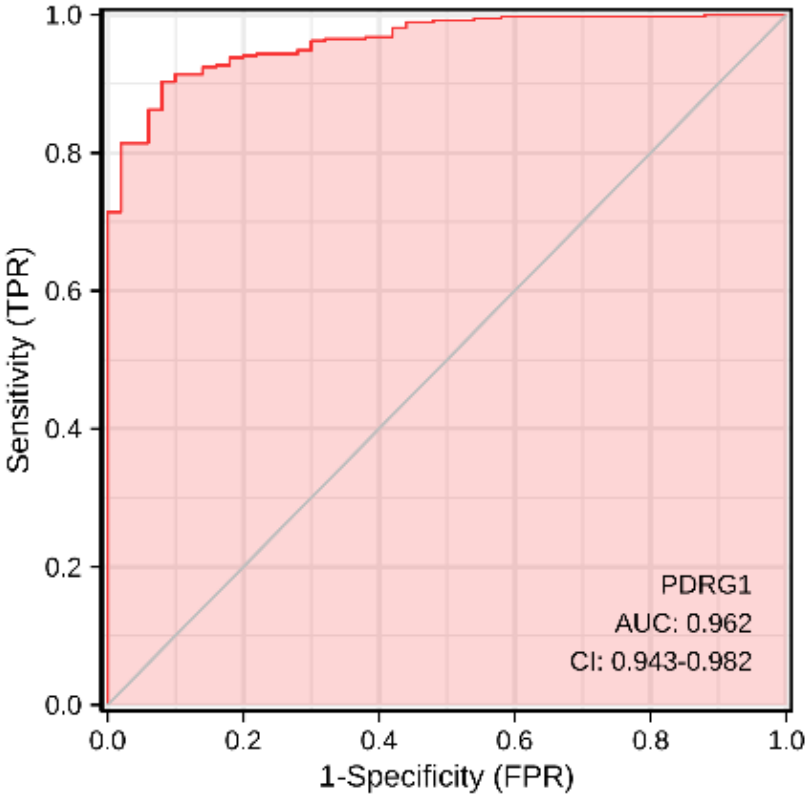

Figure 8

ROC curve of PDRG1 expression in HCC patients and healthy people; Abscissa: False Positive Rate (FPR); vertical coordinate: True Positive Rate (TPR).

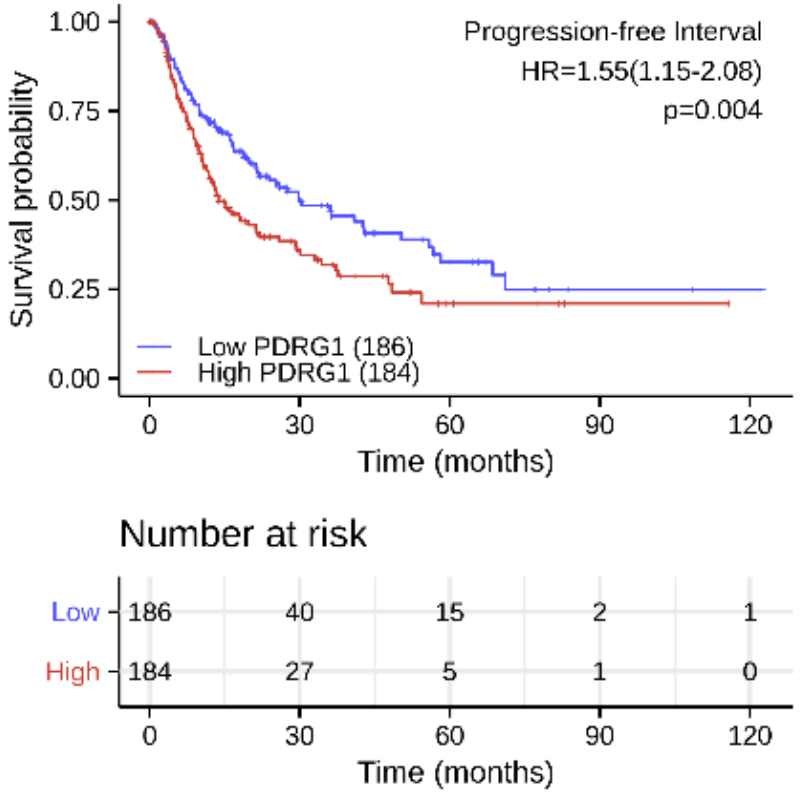

Figure 9

Kaplan-Meier Plotter of Overall Survival in HCC patients with high- or low-expression of PDRG1. The bottom half of the figure shows in risk table, recorded the number of patients who are still following at each point in time.

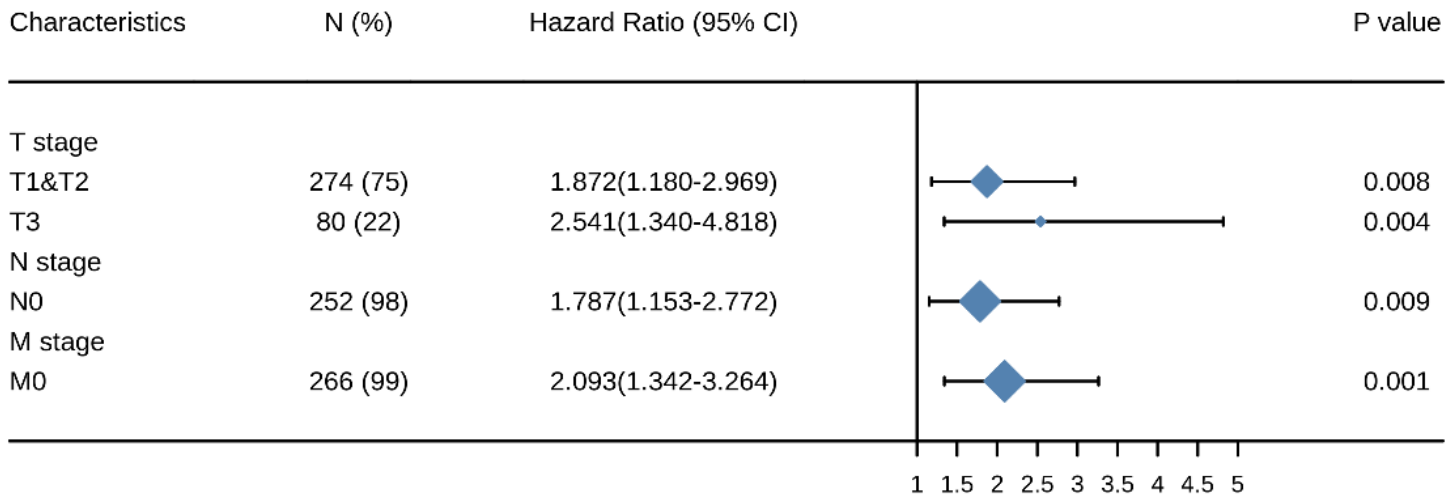

Figure 10

correlation of PDRG1 expression and Overall Survival of different clinicopathological subgroups in HCC patients.

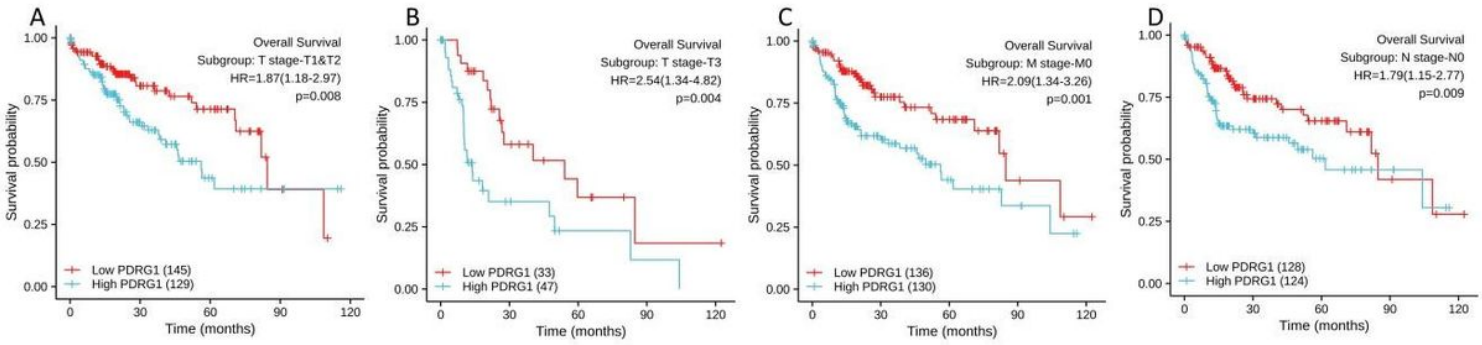

Figure 11

Kaplan-Meier Plotter showed that high expression of PDRG1 was associated with worse Overall Survival of HCC patients in different subgroups of clinicopathological factors. A. T1&T2 stage (HR□1.872, P□0.008); B. T3 stage (HR□2.541, P□0.004); C. N0 stage (HR□1.778, P□0.009); D. M0 stage (HR□2.093, P□0.001).

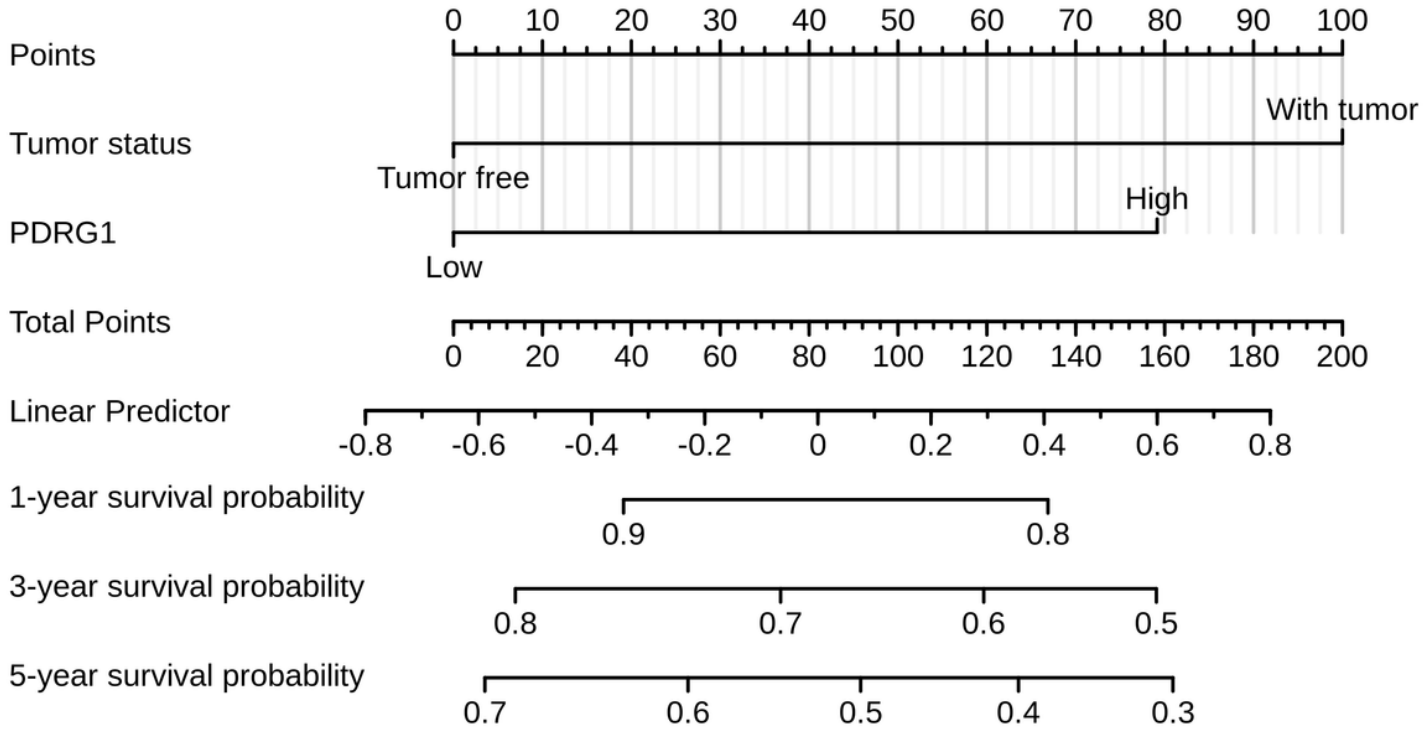

Figure 12

A nomogram predicting overall survival rates of HCC patients based on tumor stage and PDRG1

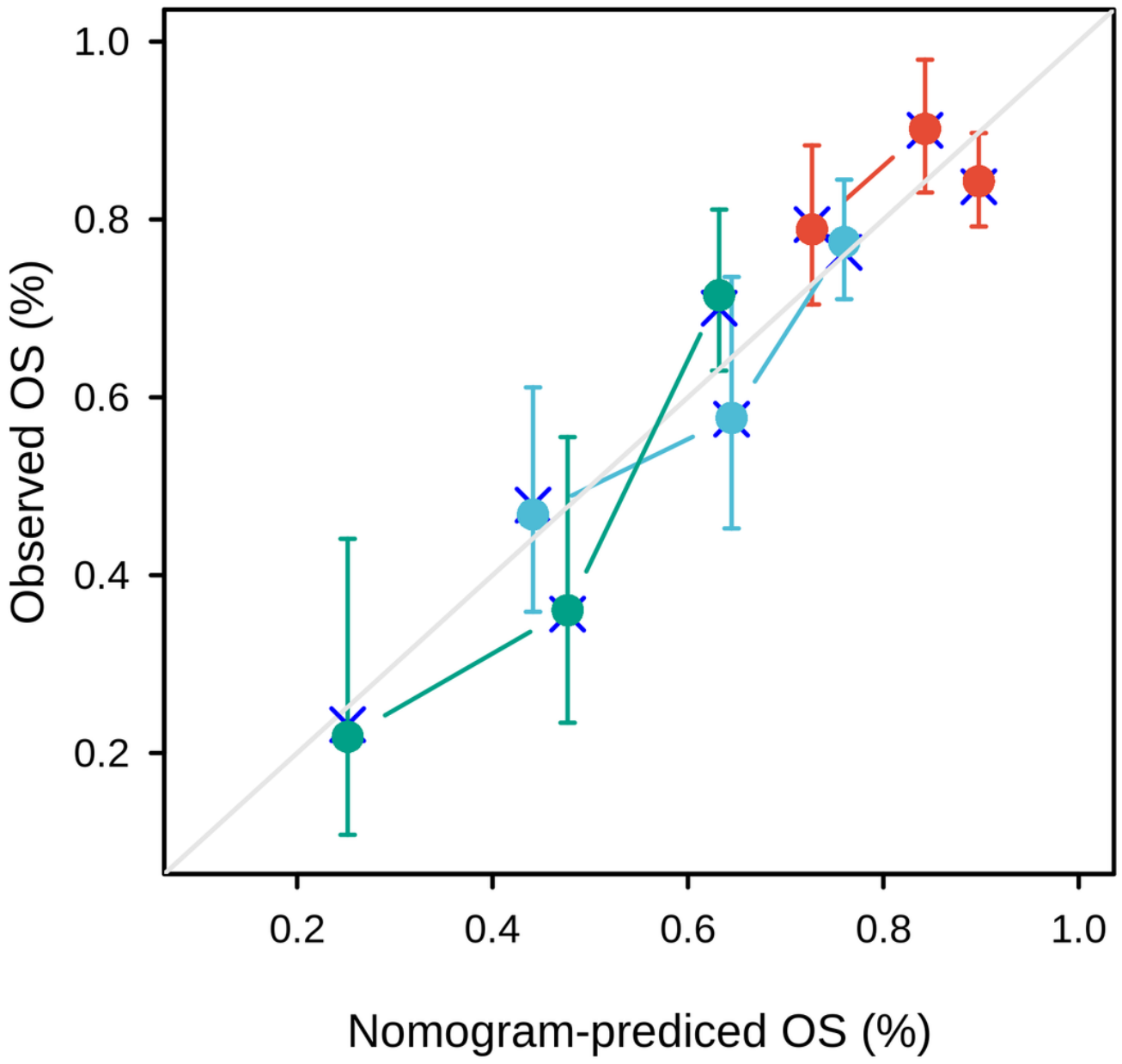

Figure 13

Calibration plot of the nomogram for predicting the probability of OS at 1, 3, and 5 years. red line: 1-year OS; blue line: 3-year OS; green line: 5-year OS; grey line: ideal line.